

**Supporting Information for**

**Ordered Structures of Alkylated Carbon Dots and Their Applications  
in Nonlinear Optics**

Keyang Yin,<sup>a,b</sup> Dandan Lu,<sup>c</sup> Wendong Tian,<sup>d</sup> Rui Zhang,<sup>d</sup> Haohai Yu,<sup>d,\*</sup> Ewa Gorecka,<sup>e</sup> Damian  
Pociecha,<sup>e</sup> Nicolas Godbert,<sup>f</sup> Junying Hao,<sup>a,\*</sup> Hongguang Li<sup>c,\*</sup>

<sup>a</sup> State Key Laboratory of Solid Lubrication, Lanzhou Institute of Chemical Physics, Chinese Academy of Sciences, Lanzhou 730000, China;

<sup>b</sup> University of Chinese Academy of Sciences, Beijing, 100049, China

<sup>c</sup> Key Laboratory of Colloid and Interface Chemistry, Shandong University, Jinan 250100, China;

<sup>d</sup> State Key Laboratory of Crystal Materials, Shandong University, Jinan 250100, China;

<sup>e</sup> Department of Chemistry, University of Warsaw, Al. Zwirki i Wigury 101, Warsaw, Poland;

<sup>f</sup> MAT\_INLAB (Laboratorio di Materiali Molecolari Inorganici) , Centro di Eccellenza CEMIF.CAL, LASCAMM CR-INSTM della Calabria, Dipartimento di Chimica e Tecnologie Chimiche, Università della Calabria, 87036 Arcavacata di Rende (CS), Italy;

## 1. Experimental details

### 1.1 Materials and Methods

The aliphatic amines, including n-dodecylamine ( $C_{12}\text{-NH}_2$ , 98%), n-tetradecylamine ( $C_{14}\text{-NH}_2$ , 96%), n-cetylamine ( $C_{16}\text{-NH}_2$ , 98%) and n-octadecylamine ( $C_{18}\text{-NH}_2$ ,  $\geq 97\%$ ) were purchased from Aladdin Biochemical Technology Co., Ltd (Shanghai, China). Chlorobenzene, ethanol, ethyl acetate were obtained from local supplier with the quality of analytical grade. All chemicals were used without further purification.

High-resolution transmission electron microscopy (HRTEM) images were recorded on a JEOL 2100 instrument operating at 200 kV. For sample preparation, a drop of sample solution ( $\sim 20 \mu\text{L}$ ) was placed on a holey-carbon coated copper grid (300 meshes) and the excess solution was soaked with a filter paper strips. The sample was then dried with an infrared lamp for 40 min before observations. Fluorescence spectra were obtained by a spectrofluorometer (LS-55). Fourier transform infrared (FTIR) spectra were recorded on a VERTEX-70/70v spectrometer (Bruker Optics, Germany) using KBr pellets. UV-vis measurements were carried out on a computer-manipulated spectrometer (UV-vis 4100, Hitachi, Japan) with a 1 cm path length quartz cell. Thermogravimetric analysis (TGA) was carried out with DSC 822e (Piscataway, NJ) under nitrogen with a scanning speed of  $10 \text{ }^\circ\text{C}\cdot\text{min}^{-1}$ . Differential scanning calorimetry (DSC) measurements were carried out on a DSC-Q2000 differential scanning calorimeter thermal analysis system (TA instrument, USA). Samples were analyzed in aluminium crucibles under a flow of nitrogen and heated at  $10 \text{ }^\circ\text{C}\cdot\text{min}^{-1}$ . An empty aluminium crucible was used as a reference. The absolute fluorescence quantum yields were obtained with a spectrofluorometer (FLSP920, Edinburgh Instruments LTD) equipped with an integrating sphere, which consists of a 120 mm inside diameter spherical cavity. 3 mL of sample solution was sealed in a quartz cell (1 cm  $\times$  1 cm) with a plug. The same volume of solvent was used as the blank sample. Small Angle X-Ray Scattering (SAXS) measurements were operated on the SAXSess mc<sup>2</sup> system (Anton Paar) with Ni-filtered Cu  $K\alpha$  radiation (1.54 Å) at 50 kV and 40 mA. Photos were taken on a digital camera (SONY DSC-TX300). X-Ray photoelectron spectroscopy (XPS) spectra were recorded on an X-ray photoelectron spectrometer (ESCALAB 250) with a monochromatized Al  $K\alpha$  X-ray source (1486.71 eV). Elemental analysis data were obtained from Vario EL CUBE (Elementar). For atomic force microscope (AFM) observations, 10  $\mu\text{L}$  sample solution was dropped on a small silica wafer and

then dried with infrared lamp for 40 min before observation in a tapping mode operating with Dimension Icon (American) at a scan frequency of 1.5 Hz. For polarized optical microscopy (POM) observations, a small amount of C dots was put onto a round quartz glass, which was covered by another round quartz glass. After gently pressed, the sample was heated to 100 °C with a speed of 20 °C·min<sup>-1</sup> controlled using Linkam LINKSYS 32 system. After holding for 5 min, the sample was cooled with a rate of ~1 °C·min<sup>-1</sup>. The texture was obtained using a Axio Scope.A1.

## 1.2 Synthesis of C dots

C dots were prepared according to our recently developed procedures. In a typical experiment, 0.05 mol aliphatic amine was added into a three-neck flask (250 mL). After removing the air by repeated vacuum-argon cycle three times, 50 mL chlorobenzene was injected, and the mixture was stirred at 50 °C for ~15 min to form a homogenous solution. Then the mixture was refluxed for 48 h. The colorless solution gradually became yellow, which indicates the formation of C dots. Chlorobenzene was removed under reduced pressure and the crude product was subjected to silica gel column chromatography using ethyl acetate as an eluant for further purification. The purified product was concentrated under reduced pressure and dried in vacuum at 40 °C for three days.

## 1.3 Evaluation of nonlinear optical properties

The nonlinear optical properties of the C dots were evaluated in the film state. A stock solution of C dots in chloroform with a concentration of 10 mg·mL<sup>-1</sup> was prepared. Then 50 μL of the stock solution was spin-coated onto a clean quartz glass with a diameter of 1 cm and a thickness of 1 mm at 2000 rpm for 30 s. After the sample was completely dried, the sample was subjected to Z-scan tests on a homemade optical measurement system employing two Rj-7620 as detectors. The power of the incident laser is adjustable from less than 1 mW to 500 mW. An illustration about the measurement system was given in the maintext. Further details can be found elsewhere.<sup>1</sup>

The data were analyzed using the model developed by Sheik-Bahae et al.<sup>2</sup> The transmittance (T) was expressed by an infinite series:

$$T = \sum_{m=0}^{\infty} \frac{-[q_0(z,0)]^m}{(m+1)^{1.5}}$$

Take the first three terms of the expression as the approximation, and the results of open aperture Z-scan measurement were polynomial fitted by the approximation:

$$T = 1 - \frac{A}{\left(1 + \left(\frac{x}{B}\right)^2\right) \times 2^{1.5}} + \frac{A}{\left(1 + \left(\frac{x}{B}\right)^2\right)^2 \times 3^{1.5}} - \frac{A}{\left(1 + \left(\frac{x}{B}\right)^2\right)^3 \times 4^{1.5}}$$

The factor  $A$  and  $B$  were obtained by polynomial fitting results, which was depended on the properties of samples.

$$A = \beta L_{eff} I_0$$

$\beta$  was third order nonlinear absorption coefficient, which was an important parameter of third order nonlinear property.  $L_{eff}$  was effective thickness, obtained by actual thickness of samples  $L$  and linear absorption  $\alpha$ :

$$L_{eff} = \frac{1 - e^{-\alpha L}}{\alpha}$$

Actual thickness was gained by AFM measurements of the samples loaded on quartz plates, while linear absorption was obtained by spectrometers. Intensity of the light source  $I_0$ , calculated by fixed repetition rate and half-peak breadth, and practical waist radius and light source power:

$$I_0 = \frac{4 \ln \sqrt{2} \cdot \left(\frac{P}{f}\right)}{\pi^{1.5} \cdot \omega_0 \tau_{half}}$$

The repetition rate ( $f$ ) and half-peak breadth ( $\tau_{half}$ ) was fixed, and power was gained by oscilloscope, waist radius ( $\omega_0$ ) was got by the fitted value of factor  $B$  and light source  $\lambda$  (1064 nm):

$$B = \frac{\pi \omega_0^2}{\lambda}$$

Finally,  $\beta$  was obtained by the equations listed above.

## 2. Additional graphs

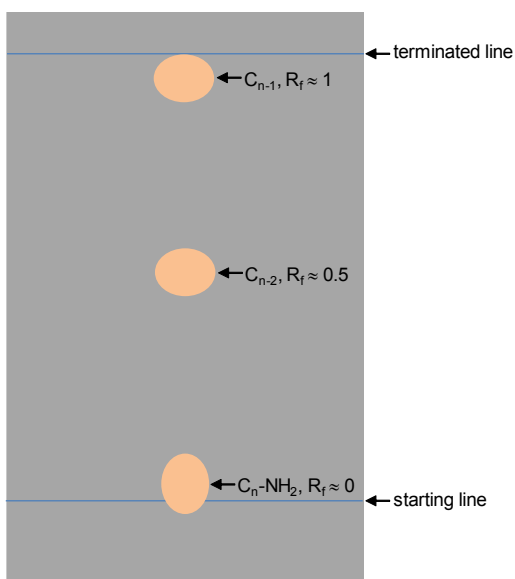


**Fig. S1** Illustration of the phenomenon observed on TLC during the purification of the reaction mixture.

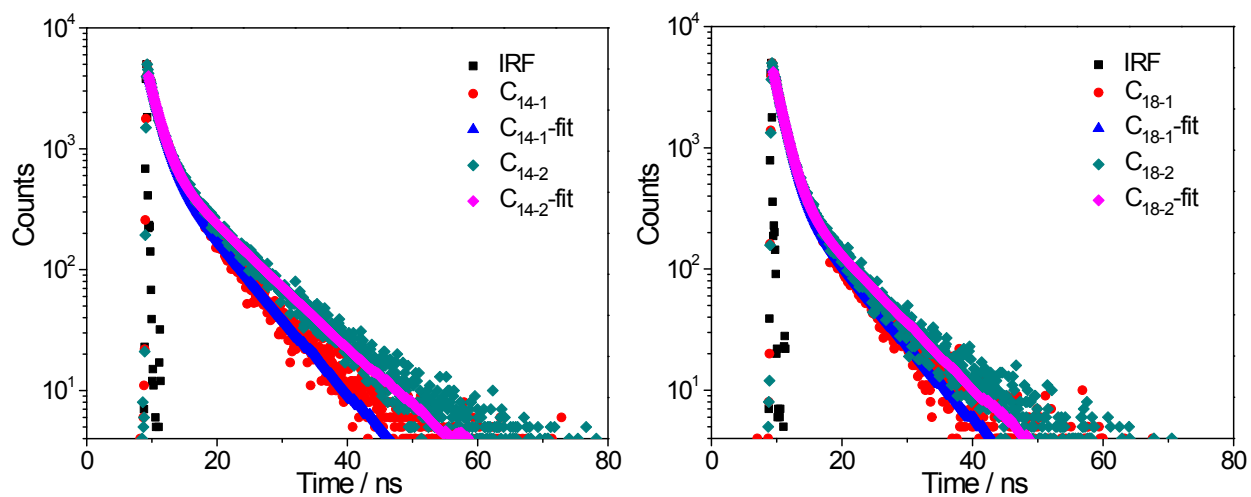


**Fig. S2** Fluorescence decays of  $C_{14-1}$ ,  $C_{14-2}$ ,  $C_{18-1}$  and  $C_{18-2}$ .

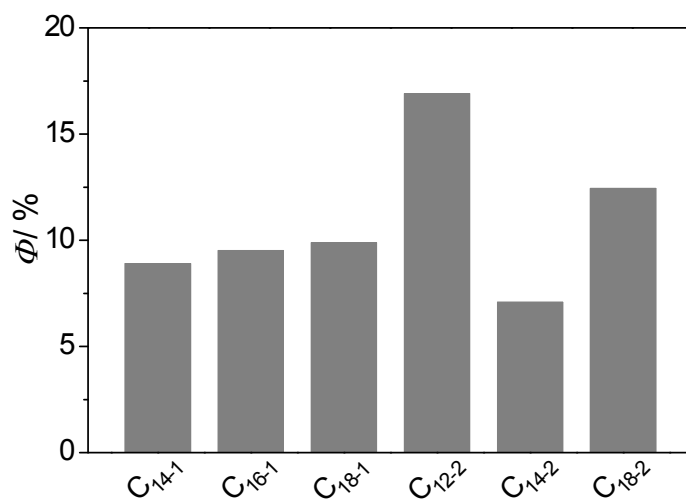


**Fig. S3** Absolute fluorescence quantum yields of the C dots.

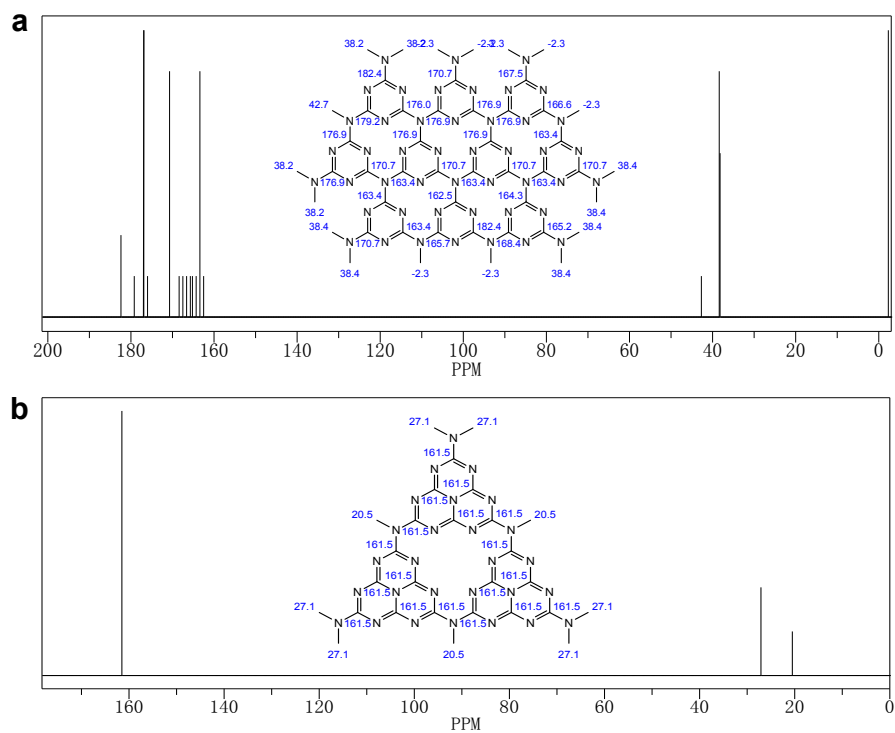


**Fig. S4** Predicted signals from  $^{13}\text{C}$  NMR by chemdraw for carbon nitride based on a) triazine and b) heptazine building blocks.

**Data notion:** The carbon nitride based on triazine gives a variety of peaks above 160 ppm, which is the expected structure in the cores of the C dots. In comparison, the carbon nitride based on heptazine only gives one peak above 160 ppm.

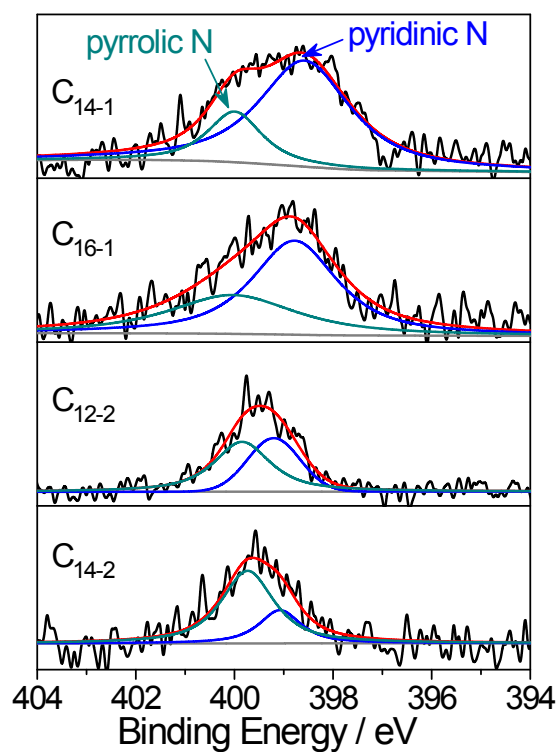


**Fig. S5** Comparison of the high-resolution N1s spectra in  $\text{C}_{14-1}$ ,  $\text{C}_{16-1}$ ,  $\text{C}_{12-2}$  and  $\text{C}_{14-2}$ .

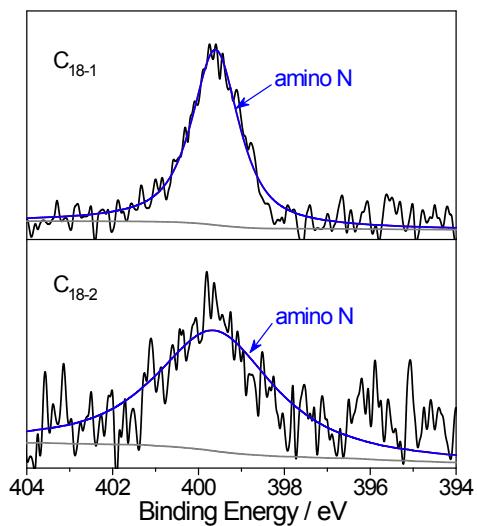


**Fig. S6** Comparison of the high-resolution N1s spectra in C<sub>18-1</sub> and C<sub>18-2</sub>.

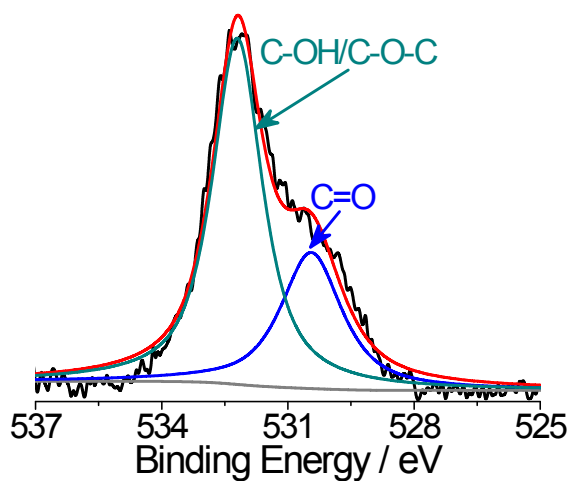


**Fig. S7** Deconvolution of the high-resolution O1s spectra in C<sub>14-1</sub>.

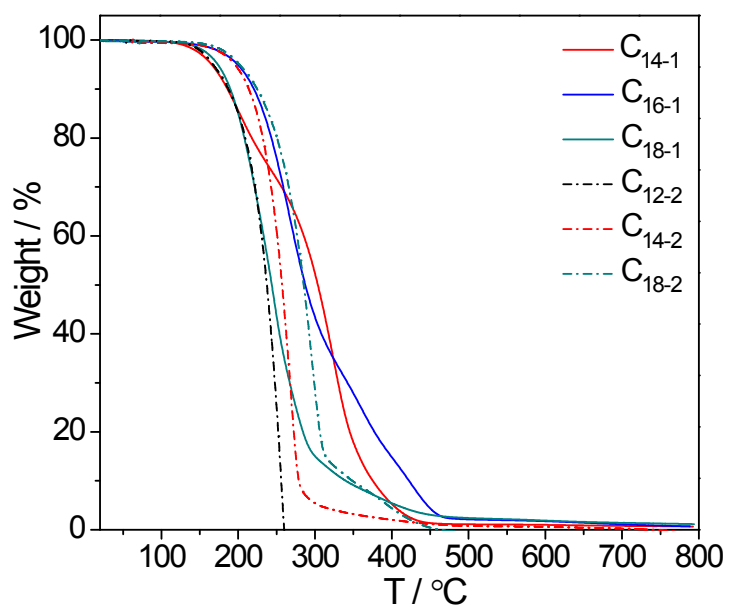


**Fig. S8** TGA traces of the C dots.

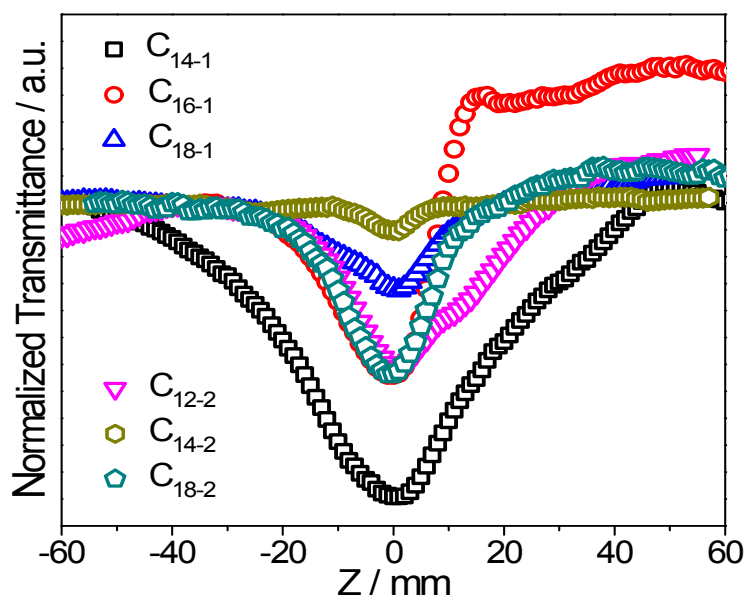


**Fig. S9** Normalized transmittance of different C dots obtained from open aperture Z scan at 5.0 mW.

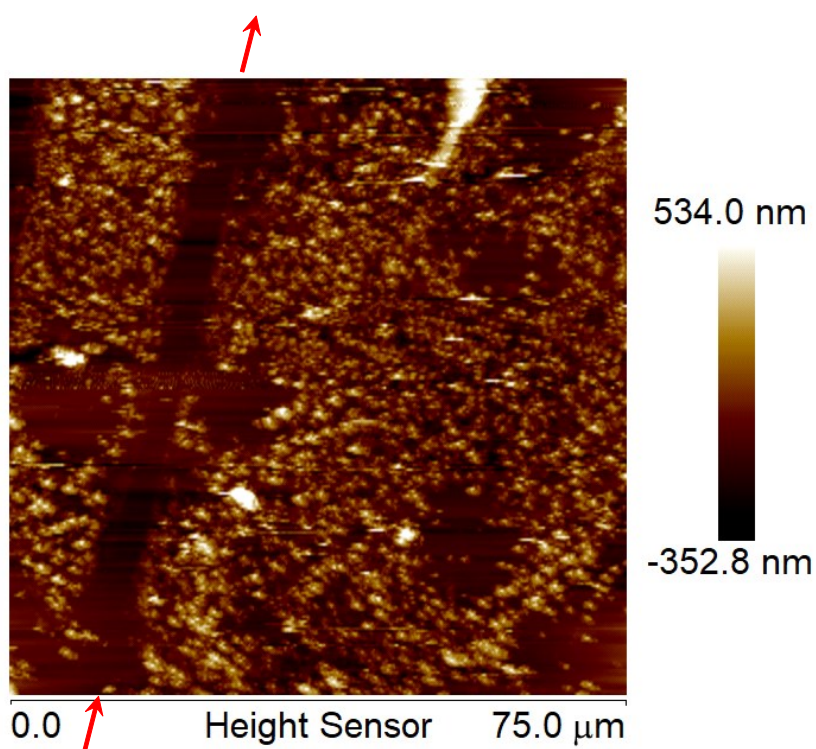


**Fig. S10** A typical AFM image of the film formed by the highly crystallized  $C_{18-2}$ . The film was scratched along the arrows to expose the substrate.



### 3. Additional tables

**Table S1.** Results of elemental analysis of the C dots and the starting materials.

	C / %	H / %	N / %	O / % <sup>a</sup>
C <sub>12-1</sub>	76.56	13.06	2.98	7.40
C <sub>12-2</sub>	73.48	13.24	6.04	7.24
C <sub>12</sub> -NH <sub>2</sub> <sup>b</sup>	77.76	14.68	7.56	0
C <sub>14-1</sub>	78.32	13.81	1.70	6.17
C <sub>14-2</sub>	74.38	13.62	5.12	6.88
C <sub>14</sub> -NH <sub>2</sub> <sup>b</sup>	79.59	14.61	5.80	0
C <sub>16-1</sub>	78.02	13.69	2.47	5.82
C <sub>16-2</sub>	76.33	14.81	4.80	4.06
C <sub>16</sub> -NH <sub>2</sub> <sup>b</sup>	78.79	14.64	6.56	0
C <sub>18-1</sub>	77.18	14.02	2.88	5.92
C <sub>18-2</sub>	76.86	13.08	3.26	6.80
C <sub>18</sub> -NH <sub>2</sub> <sup>b</sup>	80.22	14.59	5.20	0

<sup>a</sup> Calculated value.

<sup>b</sup> Theoretical value.

**Table S2.** Lifetimes from time-resolved fluorescence measurements for C<sub>14-1</sub>, C<sub>14-2</sub>, C<sub>18-1</sub> and C<sub>18-2</sub>.

	$\tau_1$ / ns	$\tau_2$ / ns	$\langle \tau \rangle$ / ns	$\chi^2$
C <sub>14-1</sub>	1.60 (56.37%)	6.64 (43.63%)	3.80	1.099
C <sub>14-2</sub>	1.58 (53.07%)	8.40 (46.93%)	4.78	1.101
C <sub>18-1</sub>	1.43 (69.38%)	6.56 (30.62%)	3.00	1.028
C <sub>18-2</sub>	1.53 (71.14%)	7.87 (28.86%)	3.36	1.045

#### 4. References

1. Wang S. Preparation and Properties of Different Dimensional Passive Optical Switches. Dissertation for doctoral degree, Shandong University.
2. Sheik-Bahae, M.; Said, A. A.; Wei, T.-H.; Hagan, D. J.; Stryland, E. W. Sensitive Measurement of Optical Nonlinearities Using a Single Beam. *IEEE J. Quantum. Elect.* **1990**, *26*, 760-769.